

Novel role of tyrosine in catalysis by human AP endonuclease 1

Sophia T. Mundle, Michael H. Fattal, Luisa F. Melo, Jean D. Coriolan,
N. Edel O'Regan, Phyllis R. Strauss*

Department of Biology, Northeastern University, 360 Huntington Avenue, Boston, MA 02115, USA

Received 28 April 2004

Available online 6 August 2004

Abstract

Apurinic/aprimidinic endonuclease (AP endo, HAP1) recognizes abasic sites in ds DNA and makes a single nick in the backbone 5' to the abasic site. In this report we examine the roles of three conserved tyrosine residues in close proximity to the active site. We show that Tyr¹²⁸ and Tyr²⁶⁹, which interact upstream and downstream of the abasic site, respectively, are involved in recognition and binding of abasic site-containing double stranded DNA. However, the two residues are not equivalent, as their effects are differentiated by changes in salt concentration. In sharp contrast, Tyr¹⁷¹ is directly involved in catalysis as well as binding. Y171F, Y171H, and Y171A all show decreased catalytic efficiencies 25,000–50,000-fold from the WT enzyme. Both imidazole and basic pH markedly stimulate the WT enzyme. Imidazole stimulates Tyr¹⁷¹ mutant enzymes when tyrosine is also present but basic pH eliminates remaining mutant activity. These results underscore the importance of tyrosines in AP endo catalysis. They render the current hypotheses regarding enzyme action unlikely and allow us to consider the possibility that the phenolate of Tyr¹⁷¹ is the nucleophile that attacks the scissile phosphate.

© 2004 Elsevier B.V. All rights reserved.

Keywords: Tyrosine; AP endonuclease 1; DNA; DNA repair; Base excision repair

1. Introduction

Tyrosine residues play important roles in a variety of enzymes. In many DNA metabolizing enzymes such as DNase I or DNA polymerase β (Pol- β) [1,2], they contribute nonspecific binding interactions by pi bonding to nucleobases and by hydrogen bonding to phosphate oxygens in the phosphodiester backbone or by stacking within the minor groove [3–5]. With DNA glycosylases such as hOGG1 or alkyl adenine glycosylase, tyrosines contribute to specificity and reactivity by stacking with an orphan residue and generating the kink

in DNA that the glycosylase recognizes [6,7]. Tyrosines play even more direct roles in various enzymatic mechanisms by serving as part of a redox active pair with histidine in cytochrome oxidase [8], extracting the hydroxyl group from ribose in ribonucleotide reductase [9], serving in the phenolate form as the catalytic base in alanine racemase [10], performing a concerted rate-limiting enolization in ketosteroid isomerase [11,12] and forming covalent DNA-protein intermediates in topoisomerases [13–15].

AP endonuclease (AP endo, also known as HAP1, APE1, and APEX) plays a key role in the removal of abasic sites from damaged DNA by generating the 3' hydroxyl required by the repair polymerase [16–18]. It initiates repair of the abasic site in ds DNA by making a single nick 5' to the phosphodeoxyribose [19–21]. In previous work we provided detailed kinetics illustrating the importance of Asp²⁸³, Asp³⁰⁸, and His³⁰⁹ in catalysis and binding. His³⁰⁹ is one of the few residues where mutation results in five orders of magnitude loss in enzymatic efficiency [22]. Here we examine the functional role of three evolutionarily conserved tyrosine residues

Abbreviations: AP endo, apurinic/aprimidinic endonuclease (HAP1, APE1, Apex); AP site, abasic site in ds DNA; BER, base excision repair; ds DNA, double-stranded DNA; CABS, (4-[cyclohexylamino]-1-butanesulfonic acid); PCR, polymerase chain reaction; PNK, polynucleotide kinase; Pol- β , DNA polymerase- β ; ROS, reactive oxygen species; RT, room temperature; TE, Tris-EDTA buffer; UDG, uracil DNA glycosylase; WT, wild type

* Corresponding author. Tel.: +1 617 373 3492; fax: +1 617 373 3724.

E-mail address: p.strauss@neu.edu (P.R. Strauss).

in the major human AP endo. The cocrystal structure with cleaved abasic site-containing ds DNA product demonstrates that Tyr¹⁷¹ lies within 4.5 Å of the 5' phosphate of the phosphodeoxyribose, while Tyr¹²⁸ and Tyr²⁶⁹ interact upstream and downstream from the abasic site, respectively [23]. The cocrystal structure with intact abasic site-containing ds DNA reveals that Tyr¹⁷¹ is 4.1 Å, even closer, to the abasic site. Tyr¹⁷¹ and Tyr¹²⁸ have been identified as important for enzymatic action [24], although no detailed kinetic analyses were performed to enable clarification of their roles. We show here that each tyrosine plays a distinct kinetic role in recognition and cleavage of abasic site containing DNA. The effects of replacing Tyr¹⁷¹ with phenylalanine, histidine or alanine are so profound that we propose that Tyr¹⁷¹ participates in the rate limiting catalytic step, even possibly as the attacking nucleophile itself.

2. Materials and methods

2.1. Site directed mutagenesis

Three tyrosine residues at positions 128, 171, and 269 were selected for mutation. Y128A, Y171A, and Y269A were generated by nested PCR site-directed mutagenesis from the WT template pXC53 plasmid containing unique *Xba*I and *Bam*HI restriction sites flanking the AP endo gene with the following primers:

Y128A	5'-GGG GCC AGT GGC <u>GTA</u> <u>GGC</u> CTG CTG-3' (<i>Stu</i> I)
	3'-CCC CGG TCA CCG <u>CAT</u> <u>CCG</u> GAC GAC-5'
Y171A	5'- <u>G</u> <u>GTA</u> <u>ACC</u> GCA GCT GTA CCT AAT GC-3' (<i>Bst</i> EII)
	3'- <u>C</u> <u>CAT</u> <u>TGG</u> CGA CGA CAT GGA TTA CG-5'
Y269A	5'-GCC <u>TAC</u> <u>ACG</u> TTT TGG ACT GCT ATG-3' (<i>Afl</i> III)
	3'-CGG <u>ATG</u> <u>TGC</u> AAA ACC TGA CGA TAC-5'

Altered nucleotides are shown in bold and new restriction sites are underlined and indicated in parentheses. The primers used to prepare the full length mutant coding sequence were:

Mut 1 5'-CTA TAG GGA GAC AAC GG-3' (*Xba*I)

Mut 2 5'-GGG AGC CAA CCT AGC TTC C-3' (*Bam*HI)

All PCR reactions were carried out in an Eppendorf Master Cycler Gradient (Westbury, NY) using a Clontech Advantage[®] cDNA Kit (Palo Alto, CA). The final PCR product consisted of the full length AP endo gene containing the desired mutation and flanked with *Xba*I and *Bam*HI restric-

tion sites. Vector lacking wild type insert, produced by digestion of pXC53 with *Xba*I/*Bam*HI (New England Biolabs, Beverly, MA) and gel purification, was mixed with the mutant AP endo gene, digested with *Bam*HI and *Xba*I and gel purified (ratio ~9:1 insert:vector). After ligation with T4 DNA ligase (New England Biolabs, Beverly, MA), ligated plasmids were amplified in DH5α *Escherichia coli* cells (Sealy Center for Molecular Biology, Galveston, TX) and sequenced to verify the presence of the desired mutation (Tufts University Core Research Facility, Boston, MA). Mutant protein was over-expressed in BL21/DE3 pLysS *E. coli* cells (Sealy Center for Molecular Biology, Galveston, TX) and purified as previously described [19].

Protein concentration was determined by Bradford dye-binding assays using bovine serum albumin as standard and a conversion factor of 0.4 to correct for AP endo concentrations [19]. This conversion factor was confirmed by comparison with protein concentration obtained using the Absorbance at 280 nm in 6 M guanidine-HCl and the theoretical extinction coefficient obtained from the amino acid sequence (<http://us.expasy.org/tools/protparam.html>). Mutants Y171F and Y171H were the gift of Dr. David Wilson III. We also showed that Wilson WT protein behaves kinetically in our assays similarly to our published results with WT AP endo (data not shown).

2.2. Enzyme assays-preparation of substrate

Enzymatic assays were performed as previously described [19]. Substrate was prepared from a 45-mer oligomer containing a single G/U pair at position 21:

5'-AGC TAC CAT GCC TGC ACG AAU TAA GCA ATT
CGT AAT CAT GGT CAT-3'

3'-TCG ATG GTA CGG ACG TGC TTG ATT CGT TAA
GCA TTA GTA CCA GTA-5'

After the U-containing strand was labeled at the 5' end with T4 polynucleotide kinase (PNK) (New England Biolabs, Beverly, MA) and heated to 70 °C to inactivate the PNK, the complementary strand was added and the solution was cooled slowly to room temperature. The double stranded, end-labeled oligomer was then treated with uracil DNA glycosylase as described [19]. Upon cleavage with AP endo, the products of the upper strand were a 5'-[³²P]-labeled 20-mer and an unlabeled 24-mer containing dRP at the 5' end. The lower strand, which was unlabeled, remained intact.

2.3. Kinetic assays

Steady state assays were performed as previously described [19] in a 5 μl volume at RT for the times indicated. Preliminary time course studies determined appropriate enzyme concentrations and time intervals. When pH studies were performed, the buffer was 25 mM CABS (4-[cyclohexylamino]-1-butananesulfonic acid). Stock CABS

(500 mM) was prepared at pH 11.3. Substrate and product were resolved by gel electrophoresis using 15% polyacrylamide in the presence of 8 M urea. The distribution of isotope was determined by PhosphorImager analysis using a Storm 840 PhosphorImager and Image Quant software (Molecular Dynamics, Sunnyvale, CA).

Steady state concentration dependence was measured using substrate concentrations between 22.5 and 1343 nM over a 30 s time interval for Y128A, a 5400 s time interval for Y171A, a 3600 s time interval for Y171F, and a 20 s interval for Y269A. We were unable to demonstrate substrate saturation for Y171H. Reaction buffer (final composition) contained 50 mM Hepes–NaOH, pH 7.5, 0.1 mM EDTA, 5 mM MgCl₂, and 150 mM NaCl (high salt) or 82 mM NaCl (low salt). During steady state experiments, final concentrations of enzyme for Y128A, Y171A, Y171F, and Y269A were 0.2, 0.2, 1, and 0.1 nM, respectively. Each experiment was repeated between 4 and 6 times with each determination performed in duplicate or triplicate. Each inhibitor experiment was repeated twice, with each determination performed in duplicate. Reactions were terminated by addition of 0.5 M EDTA to a final concentration of 87 mM. Substrate and product were resolved and quantitated as described above.

3. Results

3.1. Selection of tyrosine residues for site-directed mutagenesis

Three conserved tyrosines, Tyr¹²⁸, Tyr¹⁷¹, and Tyr²⁶⁹, were selected for site-directed mutagenesis. Fig. 1 uses the coordinates obtained from the cocrystal of the enzyme in

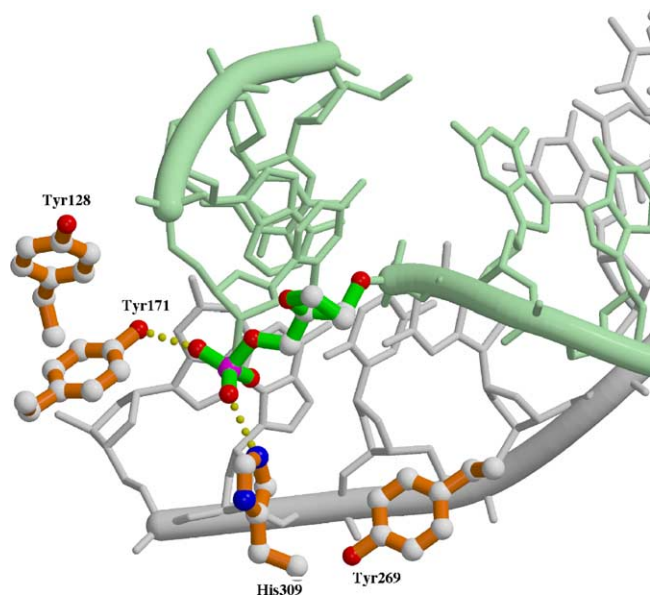


Fig. 1. Co-crystal structure of AP endo and bound product DNA showing key, selected residues. Residues Tyr¹²⁸, Tyr¹⁷¹, Tyr²⁶⁹, and His³⁰⁹ are depicted in reference to the cleaved abasic site [23].

the presence of product [23] to depict the three residues and active-site His³⁰⁹ relative to an 11-mer oligonucleotide with a single, cleaved abasic site at position 6. Both Tyr¹⁷¹ and His³⁰⁹ are 4–5 Å from the 5' phosphate of the cleaved abasic site. Tyr¹²⁸ and Tyr²⁶⁹ are further from the abasic site with the former being upstream and the latter being downstream from the cleaved abasic site. In the cocrystal with the cleaved product, the tyrosyl side chain of Tyr¹²⁸ is hydrogen bonded to Arg¹⁵⁶. However, it is 3.4 Å from one of the phosphate oxygens of cytidine C5 and 6.4 Å from the pyrimidine ring itself, which is adjacent to the abasic site and could potentially interact during binding and/or catalysis. The tyrosyl side chain of Tyr²⁶⁹ lies along the minor groove of the cleaved product but is hydrogen bonded to Asp³⁰⁸.

3.2. Tyr¹²⁸ plays an important role in recognition of abasic site-containing DNA

In the cocrystal Tyr¹²⁸ interacts upstream of the cleaved abasic site. Steady state concentration versus velocity measurements were performed between 22 and 1300 nM substrate at low and high salt. These salt conditions were chosen because we wanted to explore ionic interactions between the protein and its DNA substrate and because earlier studies [25] indicated that AP endo activity is maximal at salt concentrations between 75 and 125 mM and decreases rapidly with increasing ionic strength above 125 mM. At the two salt concentrations, K_m for WT enzyme did not change, while at high salt concentration there was a near 10-fold drop in k_{cat} (data not shown) (Table 1). The change with increased salt corresponds to a seven-fold decrease in enzyme efficiency (k_{cat}/K_m). Thus, the decrease in enzyme efficiency is easily attributed to change in binding of substrate resulting from increased ionic strength.

Table 1
Steady-state kinetic constants for tyrosine mutants^a

Mutant	Salt	k_{cat} (s ⁻¹)	K_m (nM)	k_{cat}/K_m (M ⁻¹ s ⁻¹)
WT	Low	10	100	1×10^8
	High	1.6	110	1.5×10^7
Y128A	Low	0.5	140	3×10^6
	High	0.2	108	2×10^6
Y269A	Low	1.3	165	8×10^6
	High	0.3	413	7×10^5
Y171A	Low	8×10^{-4}	360	2×10^3
	High	7×10^{-4}	310	2×10^3
Y171F	Low	9×10^{-4}	255	4×10^3
Y171H	Low	$>4 \times 10^{-3b}$	$>2000^b$	2×10^3

^a Kinetic constants for mutant and WT AP endo enzymes: kinetic constants were determined through experiments described in Section 3. K_m and k_{cat} were obtained from steady state concentration vs. velocity measurements (Fig. 2) for all mutants except Y171H.

^b Since we were unable to demonstrate saturation for Y171H, the k_{cat}/K_m for that mutant was determined from the velocity at the highest substrate concentration/ $([E][S]_{max})$. A minimum k_{cat} was calculated as $2 \times$ velocity at $[S]_{max}$, from which a minimum K_m was obtained.

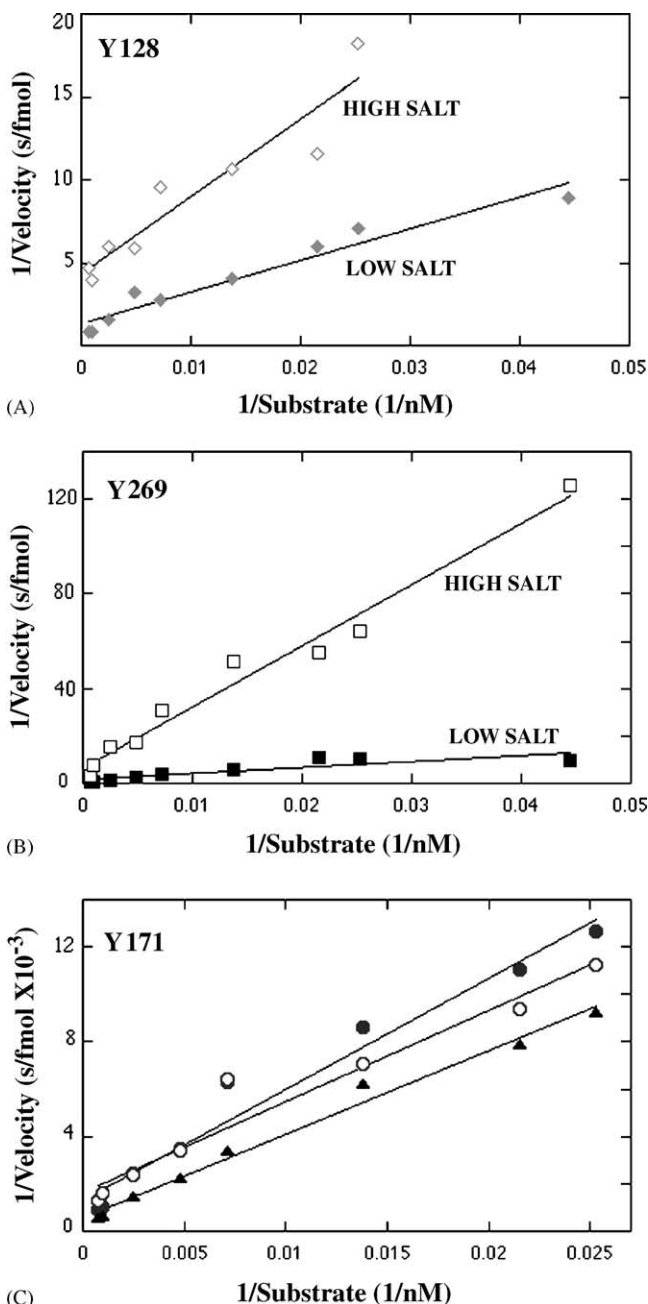


Fig. 2. Steady state concentration dependence for mutant AP endo. (A) Y128A, (◆), low salt; (◇), high salt; (B) Y269A, (■), low salt; (□), high salt; (C) Y171A, (●), low salt; Y171A, (○) high salt; Y171F, (▲), low salt. Final concentrations of enzyme for Y128A, Y171A, and Y269A were 0.2, 0.2, and 0.1, respectively. Final concentration of Y171F was 1 nM with data normalized to 0.2 nM for comparison with data from Y171A.

The results for the mutant proteins are graphically represented in Fig. 2. Fig. 2A is a Lineweaver–Burke plot of Y128A steady state results at low and high NaCl concentrations. The K_m , as shown in Table I, of Y128A at low salt concentration was 140 nM with a k_{cat} of 0.5 s^{-1} . At high salt concentration, the K_m was 108 nM with a k_{cat} of 0.2 s^{-1} . As is the case with WT AP endo, the K_m was not altered by the mutation at either salt concentration; however, the mutation

resulted in a 20-fold decrease in k_{cat} at low salt and an 8-fold decrease in k_{cat} at high salt. Compared to WT at low salt, Y128A efficiency at low salt dropped 33-fold; compared to WT at high salt, enzyme efficiency at high salt dropped 7.5-fold. Thus the effects of the mutation were more pronounced at the salt concentration that optimized enzymatic activity.

3.3. Tyr²⁶⁹, which interacts downstream of the abasic site, enhances binding and cleavage but to a lesser extent than upstream tyrosines

Fig. 2B is a Lineweaver–Burke plot of Y269A activity. At low salt concentration, Y269A exhibited a K_m of 165 nM and a k_{cat} of 1.3 s^{-1} . At high salt concentration, Y269A exhibited a K_m of 413 nM and a k_{cat} of 0.3 s^{-1} . While there was only a small change in the K_m value relative to WT enzyme, enzymatic efficiency dropped 12.5-fold at low salt and 21-fold at high salt. The salt sensitivity for steady state conditions was opposite that for Y128A.

Thus, Tyr²⁶⁹ and Tyr¹²⁸ are each involved in binding and recognizing substrate but can be differentiated by subtle changes in kinetic constants. The K_m for Y269A was higher than that for WT and Y128A; increasing salt concentration further increased the K_m for Y269A but not for Y128A. This observation is consistent with the knowledge that bulky adducts or a second abasic site located within half a helical turn and 5' to the abasic site under investigation are more debilitating to cleavage than those located downstream [26,27].

3.4. Tyr¹⁷¹ is a major player in binding and catalysis of abasic site-containing DNA

Fig. 2C is a Lineweaver–Burke plot of Y171A and Y171F steady state results. As shown in Table I, the K_m of Y171A at low salt was 360 nM with a k_{cat} of $8 \times 10^{-4} \text{ s}^{-1}$, while the K_m at high salt concentration (Table 1) was 310 nM with a k_{cat} of $7 \times 10^{-4} \text{ s}^{-1}$. Thus, there was little change in K_m and k_{cat} with the change in salt. Compared to WT, Y171A exhibited a 3-fold increase in K_m and over a 2000–12,500-fold decrease in k_{cat} . Enzyme efficiency dropped 50,000-fold to $2 \times 10^3 \text{ M}^{-1} \text{ s}^{-1}$. Similar experiments for Y171F at low salt (Fig. 2C) yielded a K_m of 255 nM, a k_{cat} of $9 \times 10^{-4} \text{ s}^{-1}$ and an enzyme efficiency of $4 \times 10^3 \text{ M}^{-1} \text{ s}^{-1}$, a decrease of 25,000-fold. Thus, the loss of the hydroxyl moiety from tyrosine was sufficient to account for the steady state results obtained with Y171A. This striking loss of enzyme efficiency could be due either to reduced binding of substrate by the mutant enzymes, to reduced catalytic activity, or to some combination of both binding and chemistry as becomes clear below. Clearly, the hydroxyl moiety of Tyr¹⁷¹ plays a prominent role in enzyme catalysis quantitatively equivalent to that played by His³⁰⁹ [22].

We were unable to obtain saturation with Y171H even at 1300 nM substrate and even when the reaction was allowed to proceed for 180 min at 1 nM enzyme. However, for enzymatic conditions substantially below the K_m concentration,

k_{cat}/K_m can be calculated by one of two methods, either from the relationship: $\text{vel} = k_{\text{cat}}/K_m[\text{E}][\text{S}]$, where $[\text{E}]$ is initial concentration of enzyme and $[\text{S}]$ is concentration of substrate [28] or from calculations arising from data obtained at the highest substrate concentration, where $k_{\text{cat}}/K_m = \text{vel} @ [\text{S}]_{\text{max}}/[\text{E}][\text{S}]_{\text{max}}$. Using the latter method, we obtain an efficiency (k_{cat}/K_m) of $2 \times 10^3 \text{ M}^{-1} \text{ s}^{-1}$, a minimum k_{cat} of $4 \times 10^{-3} \text{ s}^{-1}$ and a minimum K_m of 2000 nM. Taken together, these observations lead us to conclude that the hydroxyl moiety of Tyr¹⁷¹ may be involved in a general acid–base catalytic mechanism resulting in cleavage of the scissile phosphate in the abasic site.

3.5. Tyr¹⁷¹ is not involved in directing Mg²⁺ to the cleavage site

Since at least one crystal structure indicates that two divalent cations may participate in cleavage of the abasic site by AP endo [29], we examined whether the requirement for Mg²⁺ differed among wild type and two Tyr¹⁷¹ mutants, Y171F and Y171A (Fig. 3). Optimal Mg²⁺ concentrations occurred between 5 and 10 mM Mg²⁺ for all enzyme forms; higher Mg²⁺ (20 and 40 mM) inhibited mutants and wild type to the same extent. In short, higher Mg²⁺ concentrations did not offset the change in rate resulting from mutations in Tyr¹⁷¹. Therefore, we conclude that Tyr¹⁷¹ is unrelated to the divalent cation requirement for cleavage of the abasic site.

3.6. Imidazole enhances activity of WT enzyme markedly, enhances Y171A somewhat and fails to enhance Y171F

From theoretical calculations with THEMATICS [30,31], 4% of the hydroxyl of Tyr¹⁷¹ is likely to be in the phenolate form at any time. In an effort to resolve how Tyr¹⁷¹ is

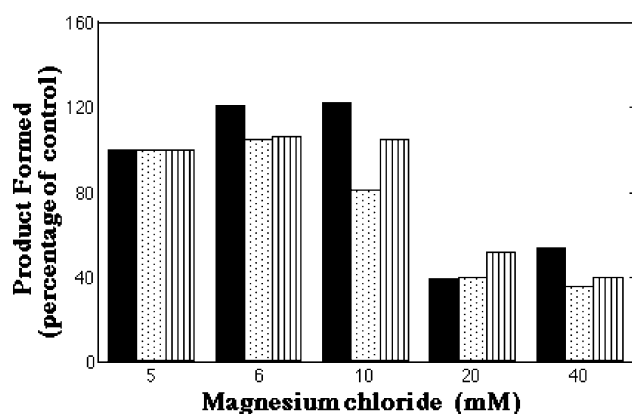


Fig. 3. Mg²⁺ dependence of wild type and Tyr¹⁷¹ mutants. Mg²⁺ was varied from 5 to 40 mM in assays for WT (■), Y171A (◻) (dots), and Y171F (▨) (vertical stripes). Each enzyme was present at 0.2 nM; substrate was maintained at 300 nM. Control WT enzyme activity at 5 mM Mg²⁺ was 54 fmol/20 s/reaction; control Y171A activity at 5 mM Mg²⁺ was 11.4 fmol/60 min/reaction; control Y171F activity at 5 mM Mg²⁺ was 8.9 fmol/60 min/reaction. These data are the average of two independent experiments.

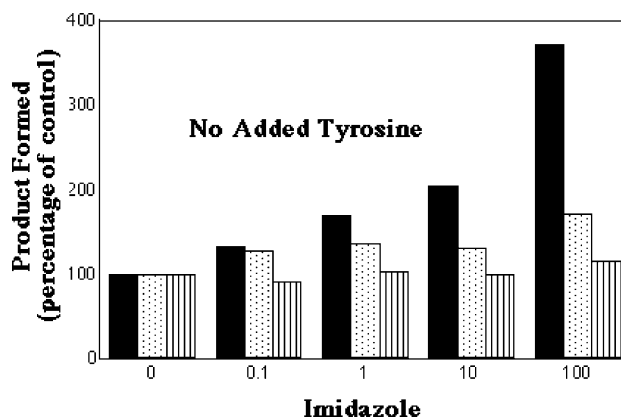


Fig. 4. In the absence of added tyrosine, imidazole enhances WT activity but has mixed effect on Tyr¹⁷¹ mutants. Increasing amounts of imidazole were added to the reaction mixtures of WT (■) and Y171A (◻) (dots) and Y171F (▨) (vertical stripes) mutants. Substrate and enzyme concentration were maintained at 300 and 0.2 nM, respectively. Wild type activity without added imidazole was 54.3 fmol/20 s/reaction, while Y171A activity without added imidazole was 10.9 fmol/60 min/reaction and Y171F control activity was 10.2 fmol/60 min/reaction. These data are the average of two independent experiments.

involved in catalysis, we examined the effects of adding imidazole to the enzymatic reaction to increase the presence of phenolate (Fig. 4). Imidazole should act as a strong base, removing protons from susceptible residues. Indeed, imidazole activated the wild type enzyme increasing activity by 272% (range: 211–327%) over the control. Imidazole at the highest concentrations enhanced Y171A by 71% (range: 35–106%) but did not enhance Y171F. These data confirm a general acid–base catalytic mechanism [32], where the most likely form initiating the reaction is the phenolate of Tyr¹⁷¹. However, they do not resolve the issue of whether the mechanism is associative or dissociative and they leave open the possibility that the phenolate of Tyr¹⁷¹ attacks the scissile phosphate directly. While a direct attack of an amino acid residue in DNA metabolizing enzymes on a phosphorous in DNA has only been reported for topoisomerases [33,34], our data are insufficient to exclude this possibility.

3.7. High pH stimulates WT enzyme but reduces mutant activity even further

High pH has been reported to inhibit AP endo cleavage activity [29]. However, the published reports were performed after the enzyme had been incubated for 2 h at elevated pH. In our hands, WT enzyme diluted in standard dilution conditions (1 μl of 125 mM NaCl, 50 mM HEPES, pH 7.4, 0.1 mM EDTA, and 50% glycerol) and mixed with 4 μl substrate in CABS, pH 11.3, to initiate the reaction at a final pH of 10.1 was stimulated close to 50% by higher pH (Fig. 5). In sharp contrast, activity of mutants Y171A, Y171F, and Y171H was reduced >90% from their control values at pH 7.4. Since higher pH will increase the percentage of Tyr¹⁷¹ in the phenolate form, these results are consistent with those obtained

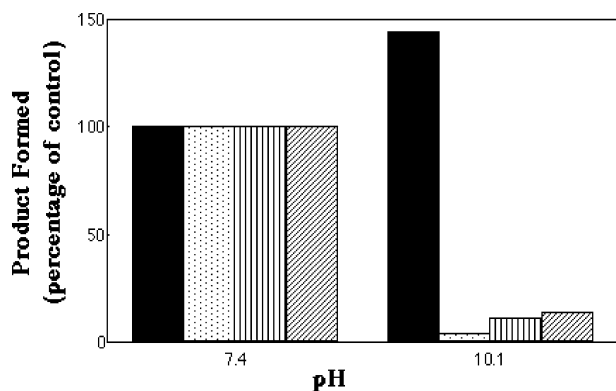


Fig. 5. Basic pH (10.1) enhances WT activity but inhibits activity of Tyr¹⁷¹ mutants. Each enzyme was diluted in standard dilution buffer (50 mM HEPES, pH 7.4, 0.1 mM EDTA, 125 mM NaCl) to 5× final concentration and maintained on ice until used. Assay mix was prepared using the standard HEPES buffer (pH 7.4) or with CABS (pH 11.3). Upon addition of 1 μl enzyme in dilution buffer, pH 7.4, to the 4 μl mix, the final pH was either 7.4 (control) or 10.1 (CABS), substrate was present at 300 nM and enzyme was added to 0.2 nM. Control WT (■) activity was 23.6 fmol/20 s/reaction, while that for Y171A (●) (dots) was 24.4 fmol/30 min/reaction, that for Y171F (|||) (vertical stripes) was 10.4/30 min/reaction and that for Y171H (▨) (oblique stripes) was 3.3 fmol/30 min/reaction. These data are the average of two independent experiments.

in the presence of imidazole described above. However, the fact that higher pH sharply DIMINISHED whatever activity had remained in the Tyr¹⁷¹ mutants, argues that solution hydroxyl is unlikely to be the moiety that attacks the scissile phosphate [23,29,35].

3.8. Imidazole in the presence of tyrosine stimulates WT as well as Y171A and Y171F mutants

The initial results with imidazole and with basic pH led us to predict that tyrosine in the phenolate form might stimulate both Tyr¹⁷¹ mutants. Tyrosine itself up to 1 mM had no effect on catalysis by AP endo (data not shown). However, when stoichiometric levels of tyrosine (24 nM, 10× molar ratio of tyrosines in AP endo during assay) were included in reaction with imidazole, wild type as well as mutants were stimulated, although the degree of stimulation of WT enzyme continued to exceed that of the mutants (Fig. 6). In this case, WT activity was stimulated by 232% (range: 211–253%), while Y171A was stimulated by 90% (range: 87–92%) and Y171F was stimulated by 90% (range: 81–103%). Although the increment is small relative to the overall loss of activity, we suggest that the phenolate form of Tyr¹⁷¹ could provide the attacking residue. Since hydroxyl ions inhibit the reaction by Tyr¹⁷¹ mutants, the most likely scenario is that the phenolate of Tyr¹⁷¹ attacks the scissile phosphorous directly.

4. Discussion

In previous publications we determined that AP endo follows a Briggs-Haldane mechanism [19]. Site directed mu-

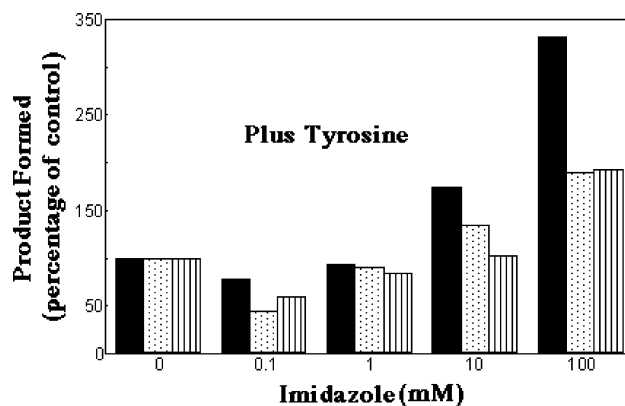


Fig. 6. In the presence of added tyrosine imidazole enhances activity of wild type and Tyr¹⁷¹ mutants. With tyrosine (24 nM) included in the reaction mixture, imidazole was varied as described in the legend to Fig. 5. Wild type (■) activity without added imidazole was 48.9 fmol/20 s/reaction, while Y171A (●) (dots) activity without added imidazole was 9.2 fmol/60 min/reaction and Y171F (|||) (vertical stripes) control activity was 5.0 fmol/60 min/reaction. These data are the average of two independent experiments.

tation of His³⁰⁹ to asparagine decreased the enzymatic efficiency more than 5 orders of magnitude and we could not obtain a binding constant by single turnover methods [22]. In this study we show that Tyr¹⁷¹ is at least as important during catalysis as His³⁰⁹. When Tyr¹⁷¹ is converted to alanine, phenylalanine or histidine, enzymatic efficiency decreases by more than 4 orders of magnitude. Therefore, the entire effect can be accounted for by loss of the tyrosyl hydroxyl. The effect is even more pronounced if Tyr¹⁷¹ is converted to histidine, since the K_m jumps more than 20-fold. Others have noted the location of Tyr¹⁷¹ in the active site and proposed that this residue plays a role in recognizing the abasic site [23,35]. Our data implicate Tyr¹⁷¹ directly in the catalytic event.

Electrostatics calculations using THEMATICs [30] have identified six residues at the active site of AP endo that are likely to be involved in catalysis [30]. Besides His³⁰⁹, examined earlier, Tyr¹⁷¹, Glu⁹⁶, Asp²¹⁰, Asp²⁸³ and Asp³⁰⁸ are predicted to contribute to the pH sensitivity of abasic-site cleavage. Earlier we showed that conversion of either Asp²⁸³ and Asp³⁰⁸ to alanine resulted in diminution of catalytic efficiency by 10–30-fold [22]. Mutation of both residues to alanine decreased enzymatic efficiency by three orders of magnitude [22]. Asp²⁸³ and Asp³⁰⁸ flank His³⁰⁹ and are likely to maintain the pK of that residue as well as its spatial orientation. Others have shown that Glu⁹⁶ and Asp²¹⁰ are important for catalysis. In the crystal structure Glu⁹⁶ binds the divalent cation [23,24,29] and Asp²¹⁰ is one of two acidic residues that flank Tyr¹⁷¹ [23,29,35,36] that could well be involved in regulating the pK of the tyrosyl hydroxyl.

Unlike Tyr¹⁷¹, Tyr¹²⁸, and Tyr²⁶⁹ are primarily involved in recognizing and binding substrate as shown by steady state measurements of site directed mutants where the residue in question was converted to alanine. That all three tyrosines

play important roles in binding substrate is consistent with the cocrystals of oligonucleotide substrate and product. In the cocrystal structure Tyr¹²⁸ spans and widens the minor groove approximately 2 Å in the presence of Mn²⁺ [23], while Tyr²⁶⁹ lies along the backbone of the helix. Tyr¹⁷¹ extends directly into the active site.

4.1. Proposed catalytic mechanism

There have been several proposed catalytic mechanisms for AP endo, based on the crystal structure of the enzyme with [23] or without [29,37] bound oligonucleotide. All proposals involve attack on the 5'-phosphate of the abasic site by an activated water molecule in analogy with cleavage by DNase I [21,23,29,38] and DNA pol I [39]. However, they neglect the critical role played by tyrosines. Our data lead us to propose that Tyr¹⁷¹ in the phenolate form not only is involved in binding abasic-site containing DNA but more importantly it can attack the scissile phosphate directly. This mechanism could easily hold for other enzymes in the Exonuclease III family, since all the critical residues are conserved [35].

The importance of His³⁰⁹ and Tyr¹⁷¹ is consistent with a general acid–base mechanism employed by many enzymes that act as phosphatases [32]. The facts that Mg²⁺ cannot overcome the defect in the Tyr¹⁷¹ mutants and that wild type and mutants respond to changes in Mg²⁺ concentrations in identical fashion excludes Tyr¹⁷¹ involvement in divalent cation binding. The fact that imidazole stimulates the wild type enzyme but has mixed effects on the mutants, coupled with electrostatic calculations that indicate that at any time 4% of Tyr¹⁷¹ is in the phenolate form [30,31], supports the hypothesis that the phenolate of Tyr¹⁷¹ is the attacking base. This leaves us with the question of whether the phenolate of Tyr¹⁷¹ attacks the scissile phosphate directly or generates the hydroxyl that will cleave the scissile phosphate. Direct attack on a scissile phosphorous has not been reported in enzymes that metabolize DNA except for topoisomerases [13,14,33,34,40,41]. However, the fact that high pH stimulates the wild type enzyme but markedly INHIBITS the Tyr¹⁷¹ mutants indicates that a hydroxyl moiety is unlikely to be involved in the rate-limiting step. Rather, we are forced to consider the possibility that the phenolate of Tyr¹⁷¹ attacks the scissile phosphate directly. We note that Pierre and Laval showed in 1981 [42] that apurinic sites in DNA were especially sensitive to peptides where one out of three residues was a tyrosine. Arg¹⁵⁶, located 4.51 Å from the tyrosyl oxygen (Fig. 7), could serve as the proton acceptor to generate the phenolate ion. Rotation of Tyr¹⁷¹ then puts the phenolate oxygen a mere 1.5 Å away from the scissile phosphorous to promote direct attack. Located on the opposite side of the scissile phosphate, the His³⁰⁹/Asp²¹⁰ pair, identified by NMR spectroscopy [43], might serve to stabilize the transition state through interaction with a non bridging oxygen and might also serve to generate the hydroxyl group that displaces Tyr¹⁷¹.

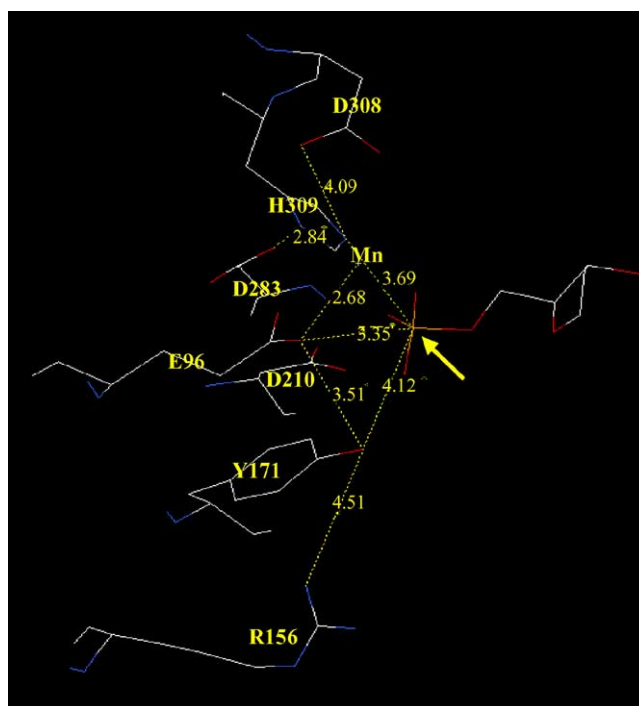


Fig. 7. Key residues within 10 Å of abasic site phosphorous. Critical amino acid residues within striking distance of the phosphorous of the abasic site are shown. The dotted lines are distances between the atoms indicated. Tyr¹⁷¹ forms a triangle with Glu⁹⁶ and the abasic site phosphorous. If Tyr¹⁷¹ is rotated around its axis, it approaches the abasic site phosphorous within 1.5 Å. Arg¹⁵⁶ provides a potential base for the hydroxyl proton of Tyr¹⁷¹. The divalent cation forms a triangle with Glu⁹⁶ and the abasic site. His³⁰⁹ is also shown with flanking Asp³⁰⁸ and Asp²⁸³ [23].

4.2. Role of divalent cations

In the cocrystal with product in the presence of Mn²⁺ [23] (Fig. 7), the divalent cation is 2.19 Å from oxygen O1 of the deoxyphosphoribose and 2.42 Å from the carboxylate oxygen of Glu⁹⁶. In the cocrystal with substrate the divalent cation is 2.08 Å from the same oxygen residue and 2.68 Å from Glu⁹⁶. Given the proximity of the divalent cation to the O1 oxygen residue in the phosphodeoxyribose of both substrate and product, it makes sense that at least one role for the divalent cation is to distort the electronic configuration of the 5' phosphate of an abasic site, resulting in a phosphorous atom that is relatively electropositive and open to attack by the phenolate residue. The possibility of a two-metal mechanism was proposed on the basis of crystallization of AP endo in the presence of Pb²⁺ [29] but discarded when liquid state NMR showed that Pb²⁺ causes a large perturbation of His³⁰⁹ that does not occur in the presence of Mg²⁺ or Ca²⁺ and that is associated with enzyme inhibition [43]. The mechanism proposed here requires only a single divalent cation.

Several confirmatory experiments would be required to substantiate this novel mechanism. First, removal of basic residues in the neighborhood of Tyr¹⁷¹ that serve as presumptive proton acceptors should have a major effect on catalysis. Second, one might predict that a two-step displacement

reaction is likely to proceed through inversion of configuration at the scissile phosphorous. Whether or not inversion occurs needs to be determined. Finally, one would ideally like to identify a covalent intermediate or a transition state analogue.

In sum, tyrosines not only play critical roles in binding and recognition of abasic site-containing oligonucleotide substrate by AP endo, one tyrosine is clearly involved intimately in the catalytic step itself.

Acknowledgements

This work was supported by NIH Grant CA72702. The authors are grateful to Dr. David Wilson III for the gift of the Y171F and Y171H mutants as well as the wild type protein prepared in his laboratory as control for his mutants and to Drs. Mary Jo Ondrechen, Robert Hanson and William Beard for critical reading of the manuscript.

References

- [1] W.A. Beard, S.A. Wilson, Structural design of a eukaryotic DNA repair polymerase: DNA polymerase β , *Mutat. Res.* 460 (2000) 231–244.
- [2] Y. Matsumoto, K. Kim, D.S. Katz, J. Feng, Catalytic center of DNA polymerase β for excision of deoxyribose phosphate groups, *Biochemistry* 37 (1998) 6456–6464.
- [3] A. Lahm, D. Suck, DNase I-induced DNA conformation. 2 angstrom structure of DNase I-octamer complex, *J. Mol. Biol.* 222 (1991) 645–667.
- [4] S.A. Weston, A. Lahm, D. Suck, X-ray structure of the DNase I-d(GGTATACC)₂ complex at 2.3 Å, *J. Mol. Biol.* 226 (1992) 1237–1256.
- [5] D.L. Wong, N.O. Reich, Identification of tyrosine-244 as the photo-cross-linking site in the DNA-EcoRI DNA methyltransferase complex by electrospray ionization mass spectrometry, *Biochemistry* 39 (2000) 15417–15420.
- [6] A.Y. Lau, M.D. Wyatt, B.J. Glassner, L.D. Samson, T. Ellenberger, Molecular basis for discriminating between normal and damaged bases by the human alkyladenine glycosylase, *AAG Proc. Natl. Acad. Sci. U.S.A.* 97 (2000) 13573–13578.
- [7] J.C. Fromme, G.L. Verdine, Structural insights into lesion recognition and repair by the bacterial 8-oxoguanine DNA glycosylase MutM, *Nat. Struct. Biol.* 9 (2002) 544–552.
- [8] D.A. Proshlyakov, M.A. Pressler, C. DeMaso, J. Leykam, D.L. DeWitt, G.T. Babcock, Oxygen activation and reduction in respiration: involvement of redox-active tyrosine 244, *Science* 290 (2000) 1588–1591.
- [9] J.M. Bollinger, D.E. Edmondson, B.H. Huynh, J. Filley, J.R. Norton, J. Stubbe, Mechanism of assembly of the tyrosyl radical-dinuclear iron cluster cofactor of ribonucleotide reductase, *Science* 253 (1991) 292–298.
- [10] M.J. Ondrechen, J.M. Briggs, J.A. McCammon, A model for enzyme–substrate interaction in alanine racemase, *J. Am. Chem. Soc.* 123 (2001) 2834–2839.
- [11] Y.K. Li, A. Kuliopulos, A.S. Mildvan, P. Talalay, Environments and mechanistic roles of the tyrosine residues of delta 5-3-ketosteroid isomerase, *Biochemistry* 32 (1993) 1816–1824.
- [12] C. Fujii, S. Morii, M. Kadode, S. Sawamoto, M. Iwami, E. Itagaki, Essential tyrosine residues in 3-ketosteroid-delta(1)-dehydrogenase from *Rhodococcus rhodochrous*, *J. Biochem. (Tokyo)* 126 (1999) 662–667.
- [13] Y.-C. Tse, K. Kirkegaard, J.C. Wang, Covalent bonds between protein and DNA, *J. Biol. Chem.* 255 (1980) 5560–5565.
- [14] J.C. Wang, DNA topoisomerases, *Annu. Rev. Biochem.* 65 (1996) 635–692.
- [15] A.I. Slesarev, K.O. Stetter, J.A. Lake, M. Gellert, R. Krah, S.A. Kozyavkin, DNA topoisomerase V is a relative of eukaryotic topoisomerase I from a hyperthermophilic prokaryote, *Nature* 364 (1993) 735–737.
- [16] E.C. Friedberg, G.C. Walker, W. Seide, *DNA Repair and Mutagenesis*, ASM Press, Washington, DC, 1995.
- [17] P.W. Doetsch, R.P. Cunningham, The enzymology of apurinic/aprimidinic endonucleases, *Mutat. Res.* 236 (1990) 173–201.
- [18] P.R. Strauss, N.E. O'Regan, Abasic site repair in higher eukaryotes, in: J. Nickoloff, M. Hoekstra (Eds.), *DNA Damage and Repair*, vol. III, Humana Press, Totowa, NJ, 2001.
- [19] P.R. Strauss, W.A. Beard, T.A. Patterson, S.H. Wilson, Substrate binding by human apurinic/aprimidinic endonuclease indicates a Briggs-Haldane mechanism, *J. Biol. Chem.* 272 (1997) 1302–1307.
- [20] J.P. Erzberger, D.M. Wilson III, The role of Mg²⁺ and specific amino acid residues in the catalytic reaction of the major human abasic endonuclease: new insights from EDTA-resistant incision of acyclic abasic site analogs and site-directed mutagenesis, *J. Mol. Biol.* 290 (1999) 447–457.
- [21] Y. Masuda, R.A.O. Bennett, B. Demple, Dynamics of the interaction of human apurinic endonuclease (Ape1) with its substrate and product, *J. Biol. Chem.* 273 (1998) 30352–30359.
- [22] J.A. Lucas, Y. Masuda, R.A.O. Bennett, N.S. Strauss, P.R. Strauss, Single turnover analysis of mutant human apurinic/aprimidinic endonuclease, *Biochemistry* 38 (1999) 4958–4964.
- [23] C.D. Mol, T. Izumi, S. Mitra, J.A. Tainer, DNA-bound structures and mutants reveal abasic DNA binding by APE1 DNA repair and coordination, *Nature* 403 (2000) 451–455.
- [24] L.H. Nguyen, D. Barsky, J.P. Erzberger, D.M. Wilson III, Mapping the protein–DNA interface and the metal-binding site of the major human apurinic/aprimidinic endonuclease, *J. Mol. Biol.* 298 (2000) 447–459.
- [25] D. Carey, P.R. Strauss, Human apurinic/aprimidinic endonuclease is processive, *Biochemistry* 38 (1999) 16553–16560.
- [26] S.V. Kolaczowski, A. Perry, A. McKenzie, F. Johnson, D.E. Budil, P.R. Strauss, A spin-labeled abasic DNA substrate for AP endonuclease, *Biochem. Biophys. Res. Commun.* 288 (2001) 722–726.
- [27] A.J. McKenzie, P.R. Strauss, Oligonucleotides with bistranded abasic sites interfere with substrate binding and catalysis by human apurinic/aprimidinic endonuclease, *Biochemistry* 40 (2001) 13254–13261.
- [28] A. Fersht, *Structure and Mechanism in Protein Science*, W.H. Freeman, New York, 1999.
- [29] P.T. Beernink, B.W. Segelke, M.Z. Hadi, J.H. Erzberger, D.M. Wilson III, B. Rupp, Two divalent metal ions in the active site of a new crystal form of human apurinic/aprimidinic endonuclease, Ape1: implications for the catalytic mechanism, *J. Mol. Biol.* 307 (2001) 1023–1034.
- [30] M.J. Ondrechen, J.G. Clifton, D. Ringe, THEMATICS: a simple computational predictor of enzyme function from structure, *Proc. Natl. Acad. Sci. U.S.A.* 98 (2001) 12473–12478.
- [31] I.H. Shehadi, Y. Yang, M.J. Ondrechen, Future directions in protein function prediction, *Mol. Biol. Rep.* 29 (2002) 329–335.
- [32] R.B. Silverman, *The Organic Chemistry of Enzyme-Catalyzed Reactions*, Academic Press, New York, 2000.
- [33] R.M. Lynn, M.A. Bjornsti, P.R. Caron, J.C. Wang, Peptide sequencing and site-directed mutagenesis identify tyrosine-727 as the active site tyrosine of *Saccharomyces cerevisiae* DNA topoisomerase I, *Proc. Natl. Acad. Sci. U.S.A.* 86 (1989) 3559–3563.
- [34] A.M. Wilstermann, N. Osheroff, Stabilization of eukaryotic topoisomerase II-DNA cleavage complexes, *Curr. Top. Med. Chem.* 3 (2003) 321–338.

- [35] M. Gorman, S. Morera, D. Rothwell, E. de La Fortelle, C. Mol, J. Tainer, I. Hickson, P. Freemont, The crystal structure of the human DNA repair endonuclease HAP1 suggests the recognition of extra-helical deoxyribose at DNA abasic sites, *EMBO J.* 16 (1997) 6548–6558.
- [36] D.G. Rothwell, B. Hang, M.A. Gorman, P.S. Freemont, B. Singer, I.D. Hickson, Substitution of Asp-210 in HAP1 (APE/Ref-1) eliminates endonuclease activity but stabilises substrate binding, *Nucleic Acids Res.* 28 (2000) 2207–2213.
- [37] C.D. Mol, C.F. Kuo, M.M. Thayer, R.P. Cunningham, J.A. Tainer, Structure and function of the multifunctional DNA-repair enzyme exonuclease III, *Nature* 375 (1995) 381–386.
- [38] S.J. Jones, A.F. Worrall, B.A. Connolly, Site-directed mutagenesis of the catalytic residues of bovine pancreatic deoxyribonuclease I, *J. Mol. Biol.* 264 (1996) 1154–1163.
- [39] L.S. Beese, T.A. Steitz, Structural basis for the 3'-5' exonuclease activity of *Escherichia coli* DNA polymerase I: a two metal ion mechanism, *EMBO J.* 10 (1991) 25–33.
- [40] J.J. Champoux, DNA topoisomerases: structure, function and mechanism, *Annu. Rev. Biochem.* 70 (2001) 369–413.
- [41] B.L. Staker, K. Hjerrild, M.D. Feese, C.A. Behnke, A.B. Burgin, L. Stewart Jr., The mechanism of topoisomerase I poisoning by a camptothecin analog, *Proc. Natl. Acad. Sci. U.S.A.* 99 (2002) 15387–15392.
- [42] J. Pierre, J. Laval, Specific nicking of DNA at apurinic sites by peptides containing aromatic residues, *J. Biol. Chem.* 256 (1981) 10217–10220.
- [43] D.F. Lowry, D.W. Hoyt, F.A. Khazi, J. Bagu, A. Lindsey, D.M. Wilson III, Investigation of the role of the histidine-aspartate pair in the human exonuclease III-like abasic endonuclease, Ape1, *J. Mol. Biol.* 329 (2003) 311–322.